Tapered fiber coupling of single photons emitted by a deterministically positioned single nitrogen vacancy center

Lars Liebermeister,[1,a)] Fabian Petersen,[1] Asmus v. Münchow,[1] Daniel Burchardt,[1] Juliane Hermelbracht,[1] Toshiyuki Tashima,[1] Andreas W. Schell,[2] Oliver Benson,[2] Thomas Meinhardt,[3,4] Anke Krueger,[3,4] Ariane Stiebeiner,[5] Arno Rauschenbeutel,[5] Harald Weinfurter,[1,6] and Markus Weber[1,6,b)]

[1]*Fakultät für Physik, Ludwig-Maximilians-Universität München, 80799 München, Germany*
[2]*Institut für Physik, Humboldt-Universität zu Berlin, 12489 Berlin, Germany*
[3]*Institut für Organische Chemie, Universität Würzburg, 97074 Würzburg, Germany*
[4]*Wilhelm Conrad Roentgen Research Center for Complex Materials Systems, Universität Würzburg, 97074 Würzburg, Germany*
[5]*Atominstitut, Technische Universität Wien, 1020 Wien, Austria*
[6]*Max-Planck-Institut für Quantenoptik, 85748 Garching, Germany*

(Received 2 September 2013; accepted 30 November 2013; published online 21 January 2014)

A diamond nano-crystal hosting a single nitrogen vacancy (NV) center is optically selected with a confocal scanning microscope and positioned deterministically onto the subwavelength-diameter waist of a tapered optical fiber (TOF) with the help of an atomic force microscope. Based on this nano-manipulation technique, we experimentally demonstrate the evanescent coupling of single fluorescence photons emitted by a single NV-center to the guided mode of the TOF. By comparing photon count rates of the fiber-guided and the free-space modes and with the help of numerical finite-difference time domain simulations, we determine a lower and upper bound for the coupling efficiency of $(9.5 \pm 0.6)\%$ and $(10.4 \pm 0.7)\%$, respectively. Our results are a promising starting point for future integration of single photon sources into photonic quantum networks and applications in quantum information science. © *2014 AIP Publishing LLC*. [http://dx.doi.org/10.1063/1.4862207]

Efficient collection of single photons radiated by a single solid state quantum emitter—like the nitrogen vacancy (NV) center in diamond[1]—is an important prerequisite for future applications in applied physical and quantum information science, like ultra-sensitive fluorescence spectroscopy and linear optical quantum computation.[2–4] A standard technique for fluorescence collection is confocal microscopy. However, when applied to defect centers in bulk diamond, total internal reflection limits the collection efficiency to few percent. Recently, the collection efficiency of NV-fluorescence has been increased by one order of magnitude by combining confocal microscopy with solid immersion lenses (SILs),[5–7] respectively, photonic nanowires.[8] In the latter system, the improvement is based on efficient coupling of NV-fluorescence photons to the strongly confined mode (HE_{11})[9–11] of diamond nanowires. For defect centers in diamond nano-crystals, tapered optical fibers (TOFs)[12] with a subwavelength diameter waist are a particularly attractive alternative platform. Due to the strong evanescent field at the surface, such TOFs promise coupling efficiencies up to 36%[13,14] and approaching unity when combined with Bragg-grating cavities.[15,16]

Until now, evanescent coupling of fluorescence photons to a single guided mode of a TOF has been achieved for various solid state quantum emitters,[17–20] molecules,[21] and laser-cooled atomic vapors.[22] To bring these emitters into the strong evanescent optical field at the surface of the nanofiber, several non-deterministic deposition techniques like dip-coating,[17,18] picoliter-dispensers,[19,20] and optical surface traps[23] have been applied. However, for real applications in quantum information science, e.g., the photonic quantum-bus mediated coupling of NV-centers in a lattice,[24] deterministic positioning of single solid state quantum emitters onto the submicron waist of a TOF with nm position control is desirable. In this Letter, we demonstrate significant steps towards deterministic coupling of a single solid state quantum emitter to a tapered optical fiber, i.e., (i) the on-demand positioning of a single diamond nano-crystal hosting a single NV-center onto the nanofiber-waist and (ii) the evanescent coupling of single fluorescence photons to a single guided mode of the TOF (see Fig. 1(a)).

Our tapered optical fiber is produced from a standard optical single mode fiber, drawn down to a waist diameter of 260 nm with a fiber-pulling-rig.[12,25] Due to the subwavelength diameter of the waist, a NV-center close to the surface of the nanofiber experiences a strong optical field[26] of the fundamental guided mode HE_{11}. This results in a small effective mode area $\mathcal{A} = [\int_A \epsilon(\vec{r})|\vec{E}(\vec{r})|^2 \, d^2\vec{r}]/[\epsilon(\vec{r}_i)|\vec{E}(\vec{r}_i)|^2]$. Here, $\epsilon(\vec{r})$ is the electric permittivity and $\vec{E}(\vec{r})$ is the electric field at a position $\vec{r}$, whereas $\epsilon(\vec{r}_i)$ and $\vec{E}(\vec{r}_i)$ are the permittivity and the field at the position $\vec{r}_i$ of the NV center. As the spontaneous emission rate into the nanofiber is given by[10] $\Gamma_{nf} = \sigma_A \Gamma_0/(2\mathcal{A})$ and as $\mathcal{A} \approx \lambda^2$ this results in strong coupling of NV-emission to the nanofiber. Here, $\sigma_A = 3\lambda^2/(2\pi)$ is the radiative atomic cross section, λ is the wavelength of the emitted photons, and Γ_0 is the spontaneous decay rate into free space modes in the absence of the nanofiber. To obtain a more quantitative prediction for our coupling efficiency, we performed numerical finite-difference time domain (FDTD) simulations with MEEP.[27] Depending on the orientation of a linearly polarized point dipole (situated

a)Email: lars.liebermeister@physik.uni-muenchen.de
b)Email: markusweber@lmu.de

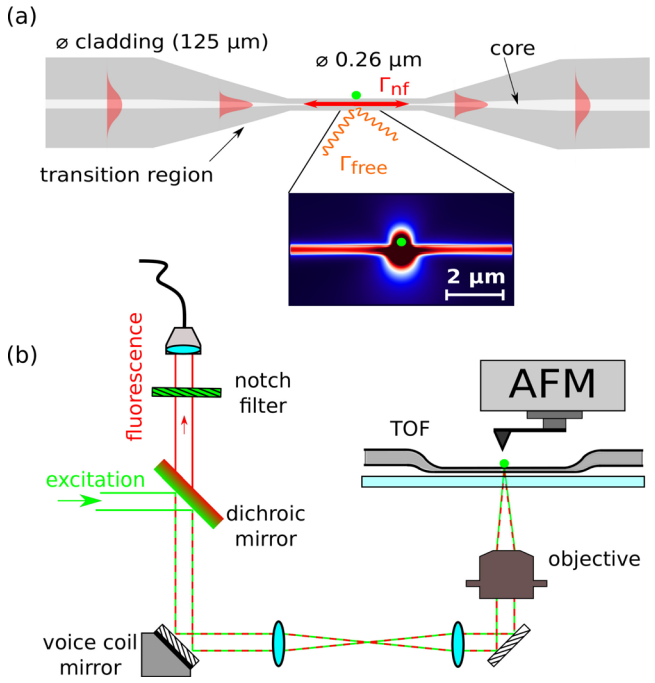

FIG. 1. (a) Schematic of evanescent coupling of single photons emitted by a single nitrogen vacancy center (hosted in a diamond nano-crystal) to a single guided mode of a TOF. Inset: FDTD simulation of the intensity distribution of a radiating NV-center coupled to the nano-fiber. (b) Schematic diagram of the experimental setup. An inverted optical confocal scanning microscope is used to analyze the fluorescence properties of individual diamond nano-crystals. In addition, an AFM is employed for *in-situ* nano-manipulation of individual crystals. Operating both microscopes at the same time allows to position a diamond nano-crystal (hosting only a single NV-center) on demand onto the apex of the optical nano-fiber.

10 nm above the nano-fiber surface), we get maximum coupling efficiencies of 27.5%, 15.6%, and 34.9% for tangential, parallel, and radial polarization, respectively.

On-demand, highly accurate picking and placing of single diamond nano-crystals are achieved using a recently introduced nano-manipulation technique,[28] based on a confocal fluorescence microscope combined with a commercial atomic force microscope (AFM) (see Fig. 1(b)). With this device, we simultaneously monitor the topography (see Fig. 2(b)) and the respective optical response (see Fig. 2(c)) of

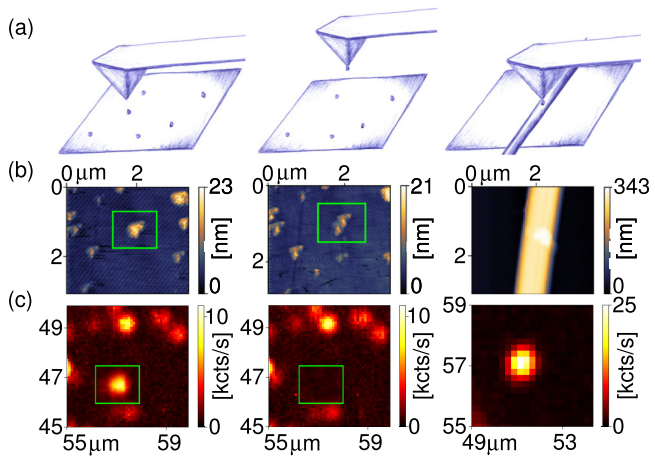

FIG. 2. (a) Schematics of the on-demand positioning of single fluorescing diamond nano-crystals onto the apex of an optical nano-fiber. (b) Topography and (c) optical scan before pick-up, after pick-up, and after placing onto the optical fiber (from left to right).

NV-centers in diamond nano-crystals before, during, and after assembly (see Fig. 2, from left to right). First, diamond nano-crystals[29] (mean diameter ≈ 25 nm) hosting single NV-centers are identified on a fused silica substrate by observing photon anti-bunching of the emitted fluorescence light. Second, the selected nano-diamond is picked up with the AFM. Third, the TOF is deposited on a clean substrate and the nano-crystal is placed onto the nano-fiber waist. Finally, the TOF is detached from the fused silica substrate.

For all optical investigations, the NV-center on the nano-fiber is excited via the confocal microscope with a continuous wave laser at a wavelength of 532 nm (perpendicular to the TOF). NV-fluorescence is collected confocally with the microscope objective (nominal numerical aperture NA = 0.75) and via the tapered optical fiber. The spectrum of the collected fluorescence photons is recorded with a CCD spectrometer with 1 nm resolution. In addition, the photon statistics of the fluorescence light is analyzed via the second-order correlation function $g^{(2)}(\tau)$, measured in a Hanbury-Brown-Twiss (HBT) configuration. Two options are possible: either with two single-photon detectors (SPDs), following a bulk beam splitter at the output fiber of the confocal microscope[1] or with two SPDs positioned at the ends of the TOF. Here, we emphasize that in the latter setting the fiber acts as intrinsic beam splitter and once photon anti-bunching is observed, it verifies the coupling of single photons to the guided mode of the TOF. Differences τ of detection times of photon pair events are recorded with a time-stamp-unit with 77 ps time resolution and stored in a histogram with a time bin width of $t_{bin} = 0.924$ ns. To obtain $g^{(2)}(\tau)$ from this delay time histogram, we divide the number of entries in each time bin by its average value for long detection time differences $\tau = 0.7 - 1.1\mu$s.

To analyze the evanescent coupling of fluorescence light emitted by a single NV-center to the guided mode of the TOF, we measured $g^{(2)}(\tau)$ for different excitation powers P (see Fig. 3(b)). For comparison, the second-order correlation function is recorded simultaneously via confocal collection (see Fig. 3(a)). Both sets of measured $g^{(2)}(\tau)$ functions are then fitted with the modified three-level model[1,30]

$$g^{(2)}(\tau) = 1 + p_f^2\left[ce^{-\frac{|\tau|}{\tau_1}} - (1+c)e^{-\frac{|\tau|}{\tau_2}}\right], \qquad (1)$$

which neglects intensity dependent deshelving of the metastable state. The parameter p_f is the probability that a detected photon event stems from a single NV-center. τ_1 describes the pump-power dependent slope of the anti-bunching dip, τ_2 governs the decay of $g^{(2)}(\tau) > 1$ for intermediate detection time differences, while c determines its amplitude. To directly quantify the influence of fluorescence, which does not stem from the NV-center on the quality of our non-classical single-photon source, we plot the fitted value of the second-order correlation function for zero detection time difference, i.e., $g^{(2)}(0) = 1 - p_f^2$ (see Fig. 4(a)). For low excitation powers, $g^{(2)}(0)$ is determined by the dark count rates of the SPDs and residual background fluorescence. Increasing P, in confocal collection, the influence of the dark count rate and the residual background fluorescence decreases, leading to almost perfect anti-bunching. In fiber-based collection, we observe an excitation power dependent increase of $g^{(2)}(0)$ from 0.26 to 0.67. This points to additional uncorrelated photons that are mainly

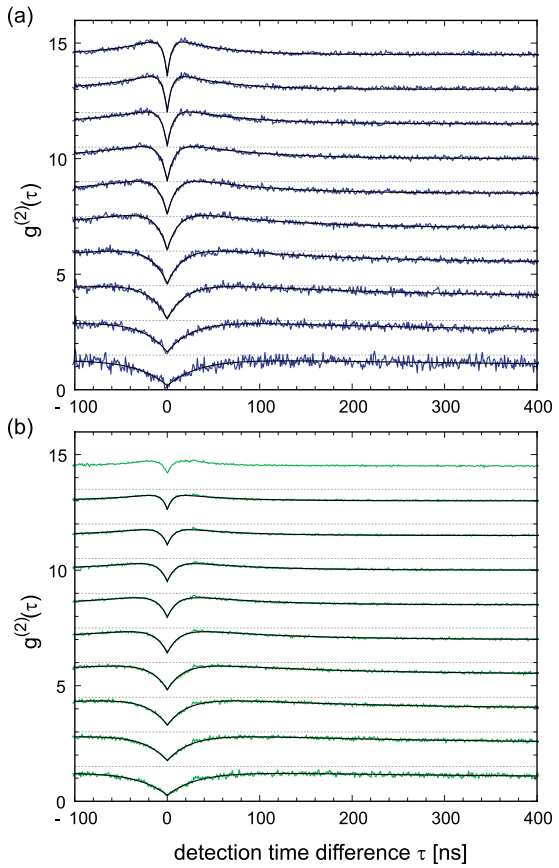

FIG. 3. Second-order correlation function $g^{(2)}(\tau)$ of fluorescence light emitted by a single NV-center for different excitation powers $P = (0.5,1.0,1.5,2,3,4,5,6,8,10)$ mW (from bottom to top), coupled to an optical nano-fiber of 260 nm diameter. The NV-center is excited perpendicular to the optical fiber via a confocal microscope. Fluorescence photons are collected (a) via the objective of the confocal microscope and (b) via coupling to the guided mode of the optical nano-fiber. The anti-bunching dip at zero detection time difference $\tau = 0$ demonstrates the non-classical character of the fluorescence light as well as the coupling of the NV-center emission to the optical nano-fiber. For better discrimination, the curves are shifted vertically by increments of 1.5.

caused by intrinsic fluorescence of the fiber core, generated by Rayleigh-scattered excitation laser light that is coupled into the nano-fiber.

As a next step, we evaluate the nano-fiber coupling efficiency $\beta = \Gamma_{nf}/(\Gamma_{nf} + \Gamma_{free})$, which is defined as the ratio of the radiative decay-rate into the nano-fiber Γ_{nf} over the total radiative decay rate $\Gamma_{rad} = \Gamma_{nf} + \Gamma_{free}$. Here, Γ_{free} is the decay rate into free-space modes in the presence of the nano-fiber. First, to determine Γ_{free}, we fit the power dependent confocal count rate (blue data points in Fig. 4(b)) with the model $kP/(P + P_{sat})$, where k is the count rate for excitation power $P \to \infty$. From this least square fit, we get a saturation power of $P_{sat} = 1.17$ mW and a free-space saturation count rate of $C_{free} = 7.70 \times 10^3\,\mathrm{s}^{-1}$. The corresponding decay rate Γ_{free} into free-space modes can be determined from C_{free} by taking into account the fraction of photons collected by the microscope objective (effective numerical aperture $\mathrm{NA}^* = 0.32 \pm 0.01$), transmission losses from the focal spot to the SPDs, and the quantum efficiency $\eta = 0.65$ of the SPDs. With the help of numerical FDTD simulations,[31] we get a lower and upper bound for Γ_{free} of $(1.7 \pm 0.1) \times 10^6\,\mathrm{s}^{-1}$ and $(1.8 \pm 0.1) \times 10^6\,\mathrm{s}^{-1}$, respectively.

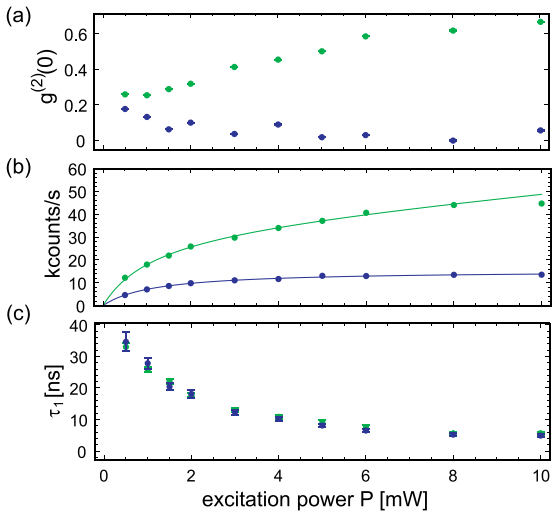

FIG. 4. (a) Second-order correlation function $g^{(2)}(0)$ at detection time difference $\tau = 0$, (b) detected count rate, and (c) fit-parameter τ_1 as a function of the excitation power P. Blue data points stem from confocal collection, whereas green data points stem from nano-fiber collection, respectively.

Next, we calculate how many single photons are scattered into the nano-fiber per second, i.e., the radiative decay rate Γ_{nf}. To determine the saturation count rate in nano-fiber collection, we fit the corresponding power dependent count rate (green data points in Fig. 4(b)) with the model $k'P/(P + P_{sat}) + mP$, taking into account an additional linear increase of the fiber background fluorescence. For this fit, P_{sat} is fixed to the value of the first fit (confocal detection and no fiber background fluorescence), resulting in a nano-fiber saturation count rate of $C_{nf} = 19.6 \times 10^3\,\mathrm{s}^{-1}$. A simple analysis shows that $\Gamma_{nf} = C_{nf}/(\eta\sqrt{T_{ges}})$, where $T_{ges} = (2.41 \pm 0.03)\%$ is the overall transmission of the TOF-system (includes the intrinsic transmission of the TOF, transmission from spectral filters, and coupling losses from the nano-fiber into detector fibers) and $\eta = 0.65$ is the quantum efficiency of the used SPDs. These values lead to $\Gamma_{nf} = (1.94 \pm 0.02) \times 10^5\,\mathrm{s}^{-1}$, resulting in a lower and upper bound for the nano-fiber coupling efficiency β of $(9.5 \pm 0.6)\%$ and $(10.4 \pm 0.7)\%$, respectively.

This value should be compared with the expected coupling efficiency of a radiating NV-center (emission wavelength $\lambda = 666$ nm, located 10 nm above the nano-fiber) coupled to a nano-fiber with 260 nm diameter. From polarization dependent excitation measurements and numerical FDTD simulations,[31] we can estimate a lower and upper bound for β, yielding $(28.78 \pm 0.03)\%$ and $(29.22 \pm 0.03)\%$, respectively. Reduction of this value by few percent is expected due to the broadband emission spectrum of the NV-center, however, cannot explain the discrepancy to our experimental finding. To clarify this contradiction, also supported by a recent experimental work with a single CdSe/ZnS nano-crystal,[17] we plan further experimental and theoretical investigations.

Concluding, as the total decay rate $\Gamma_{tot} = \Gamma_{rad} + \Gamma_{nrad}$, i.e., the sum of the radiative and nonradiative rate, can be determined from the measured second-order correlation functions for different excitation powers,[1] we furthermore can give an estimate of the internal quantum efficiency $QE = \Gamma_{rad}/\Gamma_{tot}$ of the NV-center. For small excitation powers, the

fit parameter τ_1 reaches $\tau_{tot} = 1/\Gamma_{tot} = (63 \pm 9)$ ns (see Fig. 4(c)), resulting in an upper and lower bound for the quantum efficiency *QE* of $(12.9 \pm 2.0)\%$ and $(11.8 \pm 1.8)\%$. This finding is in good agreement with recent QE-measurements from NV-centers in diamond nano-crystals of different size.[32]

In this work, we have demonstrated the on-demand positioning of a single diamond nano-crystal hosting a single NV-center onto the nanofiber-waist of a tapered optical fiber and its efficient optical coupling to a guided nano-fiber mode. The observed coupling efficiency is a promising starting point for future applications in ultra-sensitive phase,[33–35] absorption,[36] and fluorescence spectroscopy. As a single quantum emitter can shift the phase of a propagating laser beam by several degrees, this level of nonlinearity would, e.g., be sufficient to provide a useful photon-photon interaction for optical quantum information science.[37,38] Additionally, replacing the NV-center by a narrowband solid-state emitter like the SiV-center in diamond[39–41] and combining the nano-fiber with a Bragg-grating cavity[16] will pave the way towards the realization of an efficient single photon source at room temperature, an essential building block of photonic quantum computing.[2–4]

We acknowledge stimulating discussions with David Hunger and funding by the DFG through the projects FOR1493 (Diamond Materials for Quantum Application) and the excellence cluster NIM, respectively, and the BMBF through the project EPHQUAM.

[1]C. Kurtsiefer, S. Mayer, P. Zarda, and H. Weinfurter, Phys. Rev. Lett. **85**, 290 (2000).
[2]E. Knill, R. Laflamme, and G. J. Milburn, Nature **409**, 46 (2001).
[3]P. Kok, W. J. Munro, K. Nemoto, T. C. Ralph, J. P. Dowling, and G. Milburn, Rev. Mod. Phys. **79**, 135 (2007).
[4]T. Jennewein, M. Barbieri, and A. White, J. Mod. Opt. **58**, 276 (2011).
[5]J. P. Hadden, J. P. Harrison, A. C. Stanley-Clarke, L. Marseglia, Y.-L. D. Ho, B. R. Patton, J. L. O'Brien, and J. G. Rarity, Appl. Phys. Lett. **97**, 241901 (2010).
[6]P. Siyushev, F. Kaiser, V. Jacques, I. Gerhardt, S. Bischof, H. Fedder, J. Dodson, M. Markham, D. Twitchen, F. Jelezko, and J. Wrachtrup, Appl. Phys. Lett. **97**, 241902 (2010).
[7]L. Marseglia, J. P. Hadden, A. C. Stanley-Clarke, J. P. Harrison, B. Patton, Y.-L. D. Ho, B. Naydenov, F. Jelezko, J. Meijer, P. R. Dolan *et al.*, Appl. Phys. Lett. **98**, 133107 (2011).
[8]M. Babinec, B. M. Hausmann, M. Khan, Y. Zhang, J. Maze, P. R. Hemmer, and M. Loncar, Nat. Nanotechnol. **5**, 195 (2010).
[9]K.-M. C. Fu, C. Santori, P. E. Barclay, I. Aharonovich, S. Prawer, N. Meyer, A. M. Holm, and R. G. Beausoleil, Appl. Phys. Lett. **93**, 234107 (2008).
[10]P. Domokos, P. Horak, and H. Ritsch, Phys. Rev. A **65**, 033832 (2002).
[11]Q. Quan, I. Bulu, and M. Loncar, Phys. Rev. A **80**, 011810(R) (2009).
[12]A. Stiebeiner, R. Garcia-Fernandez, and A. Rauschenbeutel, Opt. Express **18**, 22677 (2010).
[13]V. V. Klimov and M. Ducloy, Phys. Rev. A **69**, 013812 (2004).
[14]F. L. Kien, S. D. Gupta, V. I. Balykin, and K. Hakuta, Phys. Rev. A **72**, 032509 (2005).
[15]F. L. Kien and K. Hakuta, Phys. Rev. A **80**, 053826 (2009).
[16]C. Wuttke, M. Becker, S. Brueckner, M. Rothhardt, and A. Rauschenbeutel, Opt. Lett. **37**, 1949 (2012).
[17]M. Fujiwara, K. Toubaru, T. Noda, H.-Q. Zhao, and S. Takeuchi, Nano Lett. **11**, 4362 (2011).
[18]T. Schroeder, M. Fujiwara, T. Noda, H. Zhao, O. Benson, and S. Takeuchi, Opt. Express **20**, 10490 (2012).
[19]R. Yalla, F. L. Kien, M. Morinaga, and K. Hakuta, Phys. Rev. Lett. **109**, 063602 (2012).
[20]R. Yalla, K. P. Nayak, and K. Hakuta, Opt. Express **20**, 2932 (2012).
[21]A. Stiebeiner, O. Rehband, R. Garcia-Fernandez, and A. Rauschenbeutel, Opt. Express **17**, 21704 (2009).
[22]K. P. Nayak, P. N. Morinaga, F. L. Kien, V. I. Balykin, and K. Hakuta, Opt. Express **15**, 5431 (2007).
[23]E. Vetsch, D. Reitz, G. Sagué, R. Schmidt, S. T. Dawkins, and A. Rauschenbeutel, Phys. Rev. Lett. **104**, 203603 (2010).
[24]F. Ciccarello, M. Paternostro, S. Bose, D. E. Browne, G. M. Palma, and M. Zarcone, Phys. Rev. A **82**, 030302(R) (2010).
[25]F. Warken, Ph.D. dissertation, University of Bonn, 2007.
[26]F. L. Kien, J. Q. Liang, K. Hakuta, and V. I. Balykin, Opt. Commun. **242**, 445 (2004).
[27]A. F. Oskooi, D. Roundy, M. Ibanescu, P. Bermel, J. D. Joannopoulos, and S. G. Johnson, Comput. Phys. Commun. **181**, 687 (2010).
[28]A. W. Schell, G. Kewes, T. Schroeder, J. Wolters, T. Aichele, and O. Benson, Rev. Sci. Instrum. **82**, 073709 (2011).
[29]Two different samples of diamond nano-crystals were used. For pick and place measurements untreated and chemically oxidized diamond nano-crystals were employed, whereas for coupling to the TOF an untreated sample from *Microdiamant* was used.
[30]C. Wang, Ph.D. dissertation, University of Munich, 2007.
[31]See supplementary material at http://dx.doi.org/10.1063/1.4862207 for polarization dependent excitation measurements and numerical FDTD simulations.
[32]A. Mohtashami and A. F. Koenderink, New J. Phys. **15**, 043017 (2013).
[33]M. Agio and V. Sandoghdar, Physica B **407**, 4086 (2012).
[34]M. Pototschnig, Y. Chassagneux, J. Hwang, G. Zumofen, A. Renn, and V. Sandoghdar, Phys. Rev. Lett. **107**, 063001 (2011).
[35]S. A. Aljunid, M. K. Tey, B. Chng, T. Liew, G. Maslennikov, V. Scarani, and C. Kurtsiefer, Phys. Rev. Lett. **103**, 153601 (2009).
[36]M. K. Tey, Z. Chen, S. A. Aljunid, B. Chng, F. Huber, G. Maslennikov, and C. Kurtsiefer, Nat. Phys. **4**, 924 (2008).
[37]W. J. Munro, K. Nemoto, and T. P. Spiller, New J. Phys. **7**, 137 (2005).
[38]J. Hwang and E. A. Hinds, New J. Phys. **13**, 085009 (2011).
[39]C. Wang, C. Kurtsiefer, H. Weinfurter, and B. Burchard, J. Phys. B **39**, 37 (2006).
[40]E. Neu, C. Arend, E. Gross, F. Guldner, C. Hepp, D. Steinmetz, E. Zscherpel, S. Ghodbane, H. Sternschulte, D. Steinmüller-Nethl, Y. Liang, A. Krueger, and C. Becher, Appl. Phys. Lett. **98**, 243107 (2011).
[41]E. Neu, F. Guldner, C. Arend, Y. Liang, S. Ghodbane, H. Sternschulte, D. Steinmüller-Nethl, A. Krueger, and C. Becher, J. Appl. Phys. **113**, 203507 (2013).